This article has been published in the Journal of the Mechanical Behavior of Biomedical Materials 2017 May 19;74:35-42. doi: 10.1016/j.jmbbm.2017.04.030.

Title: A Zinc chloride-doped adhesive facilitates sealing at the dentin interface: A confocal laser microscopy study.

Short title: A Zn-doped adhesive sealed the dentin interface.

Authors: Manuel Toledano[1*], Raquel Osorio[1], Estrella Osorio[1], Inmaculada Cabello[1], Manuel Toledano-Osorio[1], Fátima S. Aguilera[1].

Institution: [1]University of Granada, Faculty of Dentistry, Dental Materials Section.

Address: [1]University of Granada, Faculty of Dentistry, Dental Materials Section
Colegio Máximo de Cartuja s/n
18071 – Granada - Spain.

*Corresponding author: Prof. Manuel Toledano
University of Granada, Faculty of Dentistry
Dental Materials Section
Colegio Máximo de Cartuja s/n
18071 – Granada - Spain.
Tel.: +34-958243788
Fax: +34-958240809
Email: toledano@ugr.es

Abstract

The aim of this study was to understand the effect of Zn-doping of adhesives and mechanical load cycling on the micromorphology of the resin-dentin interdiffusion zone (of sound and caries affected dentin). The investigation considered two different Zn-doped adhesive approaches and evaluated the interface using confocal laser scanning microscopy. Sound and carious dentin-resin interfaces of unloaded specimens were deficiently resin-hybridized, in general. These samples showed a rhodamine B-labeled hybrid layer and adhesive layer completely affected by fluorescein penetration (nanoleakage) through the porous resin-dentin interface, but thicker after phosphoric acid-etching and more extended in carious dentin. Zn-doping promoted an improved sealing of the resin-dentin interface at dentin, a decrease of the hybrid layer porosity, and an increment of dentin mineralization. Load cycled augmented the sealing of the Zn-doped resin-dentin interfaces, as porosity and nanoleakage diminished, and even disappeared in caries-affected dentin substrata conditioned with EDTA. Sound and carious dentin specimens treated with the xylenol orange technique produced a clearly outlined fluorescence when resins were Zn-doped, due to a consistent Ca-mineral deposits within the bonding interface and inside the dentinal tubules, especially when load cycling was applied on specimens treated with Zn-doped bonding components of self-etching adhesives. Micropermeability at the resin-dentin interface diminished after combining EDTA pretreatment, $ZnCl_2$-doping and mechanical loading stimuli on restorations. It is clearly preferable to include the zinc compounds into the bonding constituents of the self-etching adhesives, instead of into the primer ingredients. The promoted new mineral segments contributed to reduce or avoid both porosity and nanoleakage from the load cycled Zn-doped resin dentin interface.

Key words: Dentin, load cycling, confocal microscopy, Zn, adhesive.

1. Introduction

Dentin represents the most common dental substrate to be used in multiple adhesive techniques for restoration (De Munck et al., 2005). Sound dentin is primarily composed of type I collagen fibrils with associated non-collagenous proteins. It forms a three-dimensional matrix that is reinforced by mineral (apatite) (Bertassoni et al., 2009), but non carious dentin is not the substrate most frequently involved in clinical dentistry. Instead, dentists usually must bond adhesives to irregular dentin substrates such as carious dentin. Carious dentin consists of two distinct layers which have different morphological and chemical structures: a superficial opaque zone of caries-infected dentin and a deeper transparent zone of caries-affected dentin (Fusayama, 1979). The latter is located adjacent to the normal dentin. Caries-infected dentin is heavily demineralized and grossly denatured, and must be removed during the clinical treatment of the dental lesion. Conversely, caries-affected dentin is partially demineralized with a predominantly intact collagen matrix. It should be preserved during clinical treatment because it is remineralizable and serves as a suitable substrate for dentin adhesion. Caries-affected dentin displays a glassy, dark yellow or slightly brown appearance. Furthermore, it exhibits a higher degree of porosity which is commonly associated with a partial lack of minerals around and within the collagen fibrils.

To promote adhesion to sound or carious dentin, a part of the mineral phase from the substrate has to be removed. The voids left by the mineral removal should be filled with the adhesive resin that undergoes complete *in situ* polymerization to form the hybrid layer (Spencer et al., 2010). Two main strategies are used to create dentin bonding. The first approach involves the use of etch-and-rinse adhesives, which require the pre-treatment of dentin with phosphoric acid (PA). This acid removes the smear layer, demineralizes the underlying dentin, and exposes a dense filigree of organic-

matrix fibrils, essentially represented by type I collagen (Breschi et al., 2010). This is followed by the application of a primer/bonding adhesive. This procedure causes a decreasing gradient of resin monomer diffusion within the acid-etched dentin which results in a phase of demineralized collagen matrix at the base of the hybrid layer (Pashley et al., 2011). Milder conditioners (*i.e.* EDTA) eliminate the smear layer and plugs, but removing less amount of calcium from dentin surface. EDTA promotes a very shallow demineralization and induces, additionally, favorable chemical modifications (Toledano et al., 2014a). Nevertheless, even with EDTA agents, it seems that a volume of demineralized and non-resin infiltrated collagen still remains at the bottom of the hybrid layer (Sencer et al., 2001). The second strategy uses self-etching adhesives. They are based on the polymerizable acidic monomers that simultaneously condition/prime and bond to the dentin, to form the hybrid complex (Tay and Pashley, 2003). With the use of this technique, it is on the whole accepted that there is less discrepancy between the depth of demineralization and the depth of resin infiltration into the dentin (Pashley et al., 2011).

Dentin adhesives should not only be long-lasting. They should protect and remineralize the resin-dentin interfaces, triggering the bioactive nature of dentin matrix, by releasing bound bioactive molecules (Burwell et al., 2012). Zinc ions inhibit matrix metalloproteases and reduce collagen degradation in demineralized dentin. Zinc has been shown to promote binding between collagen and other oligomeric matrix proteins. Protein–protein interactions are controlled by the presence of metallic cations and probably dictated by the zinc ion as the preferential ligand, even when a clear correlation between MMPs activity and clinical dentin bonding efficacy has not been yet established (Göstemeyer et al., 2016). It is known that the activity of host-derived dentin proteases is responsible for the enzymatic degradation of improperly impregnated

dentin collagen at the resin/dentin interface (Seseogullari-Dirihan et al., 2016). Therefore, a MMPs inhibitor as zinc may be of help to avoid hybrid layer degradation. Zinc may also stimulate dental remineralization (Osorio et al., 2014a). Zinc-doped adhesives may be obtained by using 10% wt ZnO or 2 wt% $ZnCl_2$. Higher solubility of ZnO when in contact with acid substrates, like some acidic non collagenous proteins (dentin matrix proteins), could also account for the effective release of zinc ions.

Occlusal stress may cause mechanical degradation and accelerate degradation within the resin–dentin interfaces (Nikaido et al., 2002; Osorio et al., 2005). At the same time, mechanical loading enhances collagen´s resistance to enzymatic degradation in demineralized dentin. It could be speculated that a relationship between those findings and some process of a partial dentin remineralization might occur. Nevertheless, degradation and remineralization studies assessing interfacial porosity and micropermeability of the bonded layer, in order to determine nanoleakage, require additional research. Fluorescence microscopy has been used to assess the interfacial morphology of the resin-dentin inter-diffusion zone and the distribution of dentin bonding agents. Fluorescent markers are incorporated into the adhesives, highlighting both the morphology and the thickness of the hybrid layer formed in thin optical sections, with minimal preparation of the sample. This technique also allows visualization of resin tag extension and determination of possible defects or alterations at the bonded restoration interface (D'Alpino et al., 2006; De Oliveira et al., 2010). Micropermeability studies have revealed important information regarding bonded layer interfacial porosity, especially in samples apparently free of interfacial gaps. The extent of the hybrid layer permeability is dependent on the penetration of adhesive components into etched dentin and on the development of porosities or gaps. Confocal laser scanning microscopy (CLSM) is capable of individually exciting different

fluorochromes by applying selective wavelengths (Griffiths et al., 1999). CLSM allows to point out the ability of fluids to penetrate the bonded interface, thus verifying the presence of micropermeability in a bonded interface (D'Alpino et al., 2006; Sauro et al., 2012). Micropermeability correlates with the presence of porosities, and so with nanoleakage. Recently, a new method to assess dentin remineralization, based on the use of a calcium-chelator fluorophore, has been proposed (Profeta et al., 2013).

The aim of this study was to analyze the morphology and micropermeability of the dentin/Zn-doped adhesive interface using two different adhesives based on different protocols of dentin conditioning, after *in vitro* mechanical loading stimuli. The null hypothesis is that nanoleakage reduction and mineral precipitation are not produced at the Zn-doped resin-dentin interface after using different protocols of dentin conditioning and mechanical loading application.

2. Material and Methods

2.1. Samples preparation

Eighty eight third molars without opposing occlusion were employed for the study. Extracted non-carious (44 specimens) and with occlusal caries (44 specimens) teeth were collected after written patients' informed consent (20 to 40 yr of age), under a protocol approved by the Institution Review Board (891/2014). Samples were stored in 0.01% (w/v) thymol at 4º C for less than 1 month. A flat mid-coronal dentin surface was exposed using a hard tissue microtome (Accutom-50; Struers, Copenhagem, Denmark) equipped with a slow-speed, water-cooled diamond wafering saw (330-CA RS-70300, Struers, Copenhagen, Denmark). The inclusion criteria for carious dentin were that the caries lesion, surrounded by sound dentin, should be limited to the occlusal surface that it extended at least half the distance from

the enamel-dentin junction to the pulp chamber. To obtain caries-affected dentin, grinding was performed by applying the combined criteria of visual examination, surface hardness employing a dental explorer, and staining by a caries detector solution (CDS, Kuraray Co., Ltd., Osaka, Japan). Using this procedure it was removed all soft, stainable, carious dentin. It was left the relatively hard, caries-affected non staining dentin, on the experimental side (Erhardt et al., 2008). A 180-grit silicon carbide (SiC) abrasive paper mounted on a water-cooled polishing machine (LaboPol-4, Struers, Copenhagem, Denmark) was used to produce a clinically relevant smear layer (Koibuchi et al., 2001).

An etch-and-rinse adhesive system, Single Bond Plus (3M ESPE, St Paul, MN, USA) (SB), was first tested. It was zinc doped by mixing the bonding resin with 20 wt% ZnO microparticles (<1 micron particle size, Panreac Química, Barcelona, Spain) (SB-ZnO) or with 2 wt% $ZnCl_2$ (Sigma Aldrich, St Louis, MO, USA) (SB-$ZnCl_2$). A two-step self-etching system, Clearfil SE Bond (Kuraray, Tokyo, Japan) (Clearfil SE) was also tested. It was zinc doped by mixing the primer of SEB (SEB·P) with 10 wt% ZnO (Panreac Química, Barcelona, Spain) (SEB·P-ZnO) or with the bonding (SEB·Bd) resin (SEB·Bd-ZnO), or by mixing the primer of SEB with 2 wt% $ZnCl_2$ (Sigma Aldrich, St Louis, MO, USA) (SEB·P-$ZnCl_2$) or with the bonding resin (SEB·Bd-$ZnCl_2$). To achieve complete dissolution of $ZnCl_2$ and dispersion of ZnO nanoparticles, adhesive mixtures were vigorously shaken for 1 min in a tube agitator (Vortex Wizard, Ref. 51075; Velp Scientifica, Milan, Italy). The complete process was performed in the dark. Employed chemicals and adhesives description are provided in Table 1.

Table 1. Materials and chemicals used in this study and respective manufacturer's application.

Product details	Basic formulation	Mode of application
Adper Single Bond Plus (SB) (3M ESPE, St Paul, MN, USA)	Bis-GMA HEMA dimethacrylates ethanol water photoinitiator system methacrylate functional copolymer of polyacrylic and polyitaconic acids	**Dentin conditioning** 37% H_3PO_4 (15 s) 0.5 M EDTA (60 s) **Adhesive application** Rinse with water Adhesive application (30 s) Light activation (15 s)
Clearfil SE Primer and Bond (SEB) (Kuraray, Japan)	***Primer*** **(SEB·P)** MDP, HEMA, camphorquinone, N, N-Diethanol-p-toluidine, water ***Bond*** **(SEB·Bd)** Bis-GMA, MDP, HEMA, camphorquinone, N, N-Diethanol-p-toluidine, silanated colloidal silica	**Adhesive application** Rinse with water Air-dry (5 s) Primer application (20 s) Air-dry (3 s) Bond application (10s) Light activation (15 s)
Zinc oxide (ZnO) (micro-particles (<1 micron particle size, Panreac Química SA, Barcelona, Spain).		
Zinc chloride 2-hydrate powder ($ZnCl_2$) (Sigma Aldrich, St. Louis, MO, USA).		
Phosphoric acid 37% (Braun Medical SA, Barcelona, Spain).		
EDTA (Sigma Aldrich, St. Louis, MO, USA).		
X-Flow™ (Dentsply, Caulk, UK)	Strontium alumino sodium fluoro-phosphorsilicate glass, di- and multifunctional acrylate and methacrylate resins, DGDMA, highly dispersed silicon dioxide UV stabilizer, ethyl-4-dimethylaminobenzoate camphorquinone, BHT, iron pigments, titanium dioxide	
SBF (pH=7.45)	NaCl 8.035 g (Sigma Aldrich, St. Louis, MO, USA). $NaHCO_3$ 0.355 g (Sigma Aldrich, St. Louis, MO, USA). KCl 0.225 g (Panreac Química SA, Barcelona, Spain). $K_2HPO_4·3H_2O$ 0.231 g, $MgCl_2·6H_2O$ 0.311 g (Sigma Aldrich, St. Louis, MO, USA) 1.0 M – HCl 39 ml (Sigma Aldrich, St. Louis, MO, USA) $CaCl_2$ 0.292 g (Panreac Química SA, Barcelona, Spain). Na_2SO_4 0.072 g (Panreac Química SA, Barcelona, Spain). Tris 6.118 g (Sigma Aldrich, St. Louis, MO, USA) 1.0 M – HCl 0–5 ml (Panreac Química SA, Barcelona, Spain).	

Abbreviations: Bis-GMA: bisphenol A diglycidyl methacrylate; HEMA: 2-hydroxyethyl methacrylate; MDP: Methacryloyldodeylphosphate; DGDMA: diethyleneglycol dimethacrylate phosphate; BHT: butylated hydroxytoluene; H_3PO_4: phosphoric acid; EDTA: ethylenediaminetetraacetic acid; SBF: simulated body fluid; NaCl: sodium chloride; $NaHCO_3$: sodium bicarbonate; KCl: potassium chloride; $K_2HPO_4·3H_2O$: potassium phosphate dibasic trihydrate; $MgCl_2·6H_2O$: magnesium chloride hexahydrate; HCl: hydrogen chloride; $CaCl_2$: Calcium chloride; Na_2SO_4: sodium sulfate; Tris: tris(hydroxylmethyl) aminomethane.

The specimens were divided into the following main groups (n=4) based on the tested adhesive systems and dentin-etching procedure: (i) SB was applied on 37% phosphoric acid (PA) treated dentin, 15 s (PA+SB); (ii) SB was applied on EDTA-treated dentin, 0.5 M, 60 s (EDTA+SB); (iii) SB-ZnO was applied on 37% PA treated dentin (PA+SB-ZnO); (iv) SB-ZnO was applied on EDTA-treated dentin, 0.5 M, 60 s (EDTA+SB-ZnO); (v) SB-$ZnCl_2$ applied on 37% (PA+SB-$ZnCl_2$); (vi) SB-$ZnCl_2$ applied on EDTA-treated dentin, 0.5 M, 60 s (EDTA+SB-$ZnCl_2$). Concerning the self-etching adhesives, the specimens were divided into the following main groups (n=4): (i): Clearfil SEB (SEB); (ii): SEB·P-ZnO was applied followed by the resin bonding, SEB·Bd, (SEB·P-ZnO); (iii): SEB·P-$ZnCl_2$ was applied followed by de resin bonding, SEB·Bd, (SEB·P-$ZnCl_2$); (iv): SEB·Bd-ZnO was applied after the primer, SEB·P, placement (SEB·Bd-ZnO), and (v): SEB·Bd-$ZnCl_2$ was applied after the primer, SEB·P, placement (SEB·Bd-$ZnCl_2$). Each experimental group had 4 sound and 4 caries-affected specimens.

The bonding procedures were performed in moist sound or caries-affected dentin following the manufacturer´s instructions. A flowable resin composite (X-Flow™, Dentsply, Caulk, UK) was placed incrementally in five 1 mm layer and light-cured with a Translux EC halogen unit (Kulzer GmbH, Bereich Dental, Wehrheim, Germany) for 40 s.

2.2. Confocal microscopy evaluation

Previous to adhesive application, bond resins were doped with 0.05 wt% Rhodamine-B (RhB: Sigma-Aldrich Chemie Gmbh, Riedstr, Germany). In 32 specimens, the pulpal chamber was filled with 1 wt% aqueous/ethanol fluorescein (Sigma-Aldrich Chemie Gmbh, Riedstr, Germany) for 3 h (Sauro et al., 2012; Toledano et al., 2013a). The rest of the molars were immersed in 0.5 wt% xylenol orange solution

(Xo: Sigma-Aldrich Chemie Gmbh, Riedstr, Germany), excited at 514-nm for 24 h at 37 ºC (pH 7.2). The latter is a calcium-chelator fluorophore commonly used in hard tissues remineralization studies, due to its ability to form complexes with divalent calcium ions (Profeta et al., 2013). Specimens were copiously rinsed with water and treated in an ultrasonic water bath for 2 min. The specimens were cut in resin-dentin slabs and polished using ascending grit SiC abrasive papers (#1200 to #4000) on a water-cooled polishing device (Buehler-MetaDi, Buehler Ltd. Lake Bluff, IL, USA). A final ultrasonic cleaning (5 min) concluded the specimen preparation. Analysis of bonded interfaces were performed by dye assisted confocal microscopy evaluation (CLSM), and attained by using a confocal laser scanning microscope (SP5 Leica, Heidelberg, Germany) equipped with a 20x, 40x and 60x oil immersion lenses. Fluorescein was activated by blue light (488-495 nm) and emited yellow/green (520 nm), while the ultramorphology evaluation (resin-diffusion) was executed using Rhodamine excitation laser. Rhodamine was excited using green light (540 nm) and emited red in color (590 nm). CLSM images were obtained with a 1 μm z-step to optically section the specimens to a depth up to 12-10 μm below the surface. The z-axis scans of the interface surface was arbitrarily pseudo-colored by the same operator for better exposure and compiled into single projections using the Leica image-processing software SP2 (Leica, Heidelberg, Germany). The resolution of CLSM images was 1024 x 1024 pixels. Five optical images were randomly captured from each resin-dentin interface, and micrographs representing the most common features of nanoleakage observed along the bonded interfaces were selected (Profeta et al., 2013; Toledano et al., 2013b). Three specimens from each subgroup were immersed. Fluorescences were or not separated into spectral regions, allowing that the operator has a full control of the region of the light spectrum directed to each channel.

2.3. Mechanical loading

Specimens were sectioned, and one half of each specimen was submitted to mechanical loading. To proceed with the mechanical cycling test, teeth were mounted in the load cycling machine [100,000 cycles, 3 Hz, 49 N (load range, 59-10 N)] (S-MMT-250NB; Shimadzu, Tokyo, Japan). The cycling compressive was applied to the flat resin composite build-ups using a 5-mm diameter spherical stainless steel plunger, while immersed in simulated body fluid (SBF) (Table 1). Specimens were then immersed in SBF, in order to complete a 24 h storage period. Non-loaded specimens were stored in SBF for 24 h. The experiment was done at room temperature controlled to 25 ºC. The groups of study are displayed in Table 2.

Table 2. Table of cases

Figure number	Dentin	Dentin pre-treatment	Adhesive	Load	Dye
1A	SD	PA-etch	SB	No	Rd/Fl
1B	SD	EDTA-etch	SB	No	Rd/Fl
1C	SD	Self-etch	SEB	No	Rd/Fl
2A	SD	PA-etch	SB-ZnO	No	Rd/Fl
2B	SD	PA-etch	SB-ZnO	Yes	Rd/Fl
2C	SD	PA-etch	SB-$ZnCl_2$	No	Rd/Fl
2D	SD	PA-etch	SB	Yes	Rd/Xo
3A	SD	EDTA-etch	SB-ZnO	No	Rd/Fl
3B	SD	EDTA-etch	SB	Yes	Rd/Xo
3C	SD	EDTA-etch	SB-$ZnCl_2$	No	Rd/Fl
3D	SD	EDTA-etch	SB-$ZnCl_2$	No	Rd/Xo
4A	CAD	PA-etch	SB	No	Rd/Fl
4B	CAD	PA-etch	SB	Yes	Rd/Fl
4C	CAD	PA-etch	SB-ZnO	No	Rd/Fl
4D	CAD	PA-etch	SB-ZnO	Yes	Rd/Xo
4E	CAD	PA-etch	SB-$ZnCl_2$	No	Rd/Fl
4F	CAD	PA-etch	SB-$ZnCl_2$	Yes	Rd/Fl
5A	CAD	EDTA-etch	SB	No	Rd/Fl
5B	CAD	EDTA-etch	SB	Yes	Rd/Xo
5C	CAD	EDTA-etch	SB-$ZnCl_2$	No	Rd/Fl
5D	CAD	EDTA-etch	SB-$ZnCl_2$	Yes	Rd/Fl
6A	SD	Self-etch	SEB·P-$ZnCl_2$	No	Rd/Fl
6B	SD	Self-etch	SEB·P-$ZnCl_2$	Yes	Rd/Fl
6C	SD	Self-etch	SEB·Bd-$ZnCl_2$	No	Rd/Fl
6D	SD	Self-etch	SEB·Bd-$ZnCl_2$	Yes	Rd/Fl
6E	SD	Self-etch	SEB·P-ZnO	Yes	Rd/Xo
6F	SD	Self-etch	SEB·Bd-ZnO	Yes	Rd/Xo
6G	SD	Self-etch	SEB·Bd-$ZnCl_2$	Yes	Rd/Xo
7A	CAD	Self-etch	SEB·P-ZnO	No	Rd/Fl
7B	CAD	Self-etch	SEB·Bd-ZnO	Yes	Rd/Fl
7C	CAD	Self-etch	SEB·P-ZnO	Yes	Rd/Xo
7D	CAD	Self-etch	SEB·Bd-ZnO	Yes	Rd/Xo
7E	CAD	Self-etch	SEB·P-$ZnCl_2$	Yes	Rd/Xo
7F	CAD	Self-etch	SEB·Bd-$ZnCl_2$	Yes	Rd/Xo

Abreviations: SB: Adper Single Bond Plus; PA: Phosphoric Acid; EDTA: ethylenediaminetetraacetic acid; SEB: Clearfil SE Primer and Bond; Rd: Rhodamine B; Fl: fluorescein; Xo: Xylenol orange; SB-ZnO: Single Bond adhesive-ZnO doped; SB-$ZnCl_2$: Single Bond adhesive-$ZnCl_2$ doped; SEB·P-$ZnCl_2$: Clearfil SE Primer-$ZnCl_2$ doped; SEB·P-ZnO: Clearfil SE Primer-ZnO doped; SEB·Bd-$ZnCl_2$: Clearfil SE Bonding-$ZnCl_2$ doped; SEB·Bd-ZnO: Clearfil SE Bonding-ZnO doped; SD: sound dentin; CAD: caries-affected dentin.

3. Results and discussion

When carious dentin was pretreated with EDTA and Zn-doped adhesives infiltrated the substrate, load cycling of restorations reduced both porosity and nanoleakage and augmented mineralization at the resin-dentin interface. Based on the results obtained in this study, the null hypothesis that nanoleakage reduction and mineral precipitation are not produced at the Zn-doped resin-dentin interface after using different protocols of dentin conditioning and mechanical loading application, must be rejected. Load cycling applied on the resin-dentin interfaces produced by two different adhesives and based on different protocols of dentin conditioning, after *in vitro* mechanical loading stimuli, promoted advance of sealing and mineralization of the resin-dentin interfaces.

Figures 1 to 7 are showing the CLSM images of the resin-dentin interfaces attained in the experimental groups.

3.1. Zn-doped etch-and rinse adhesives, in PA treated dentin

In general, the CLSM analysis revealed that resin-dentin interfaces of undoped and unloaded specimens obtained with phosphoric acid and Single Bond adhesive (PA+SB) were deficiently resin-hybridized in both sound dentin (Fig. 1A) and caries-affected dentin (Fig. 4A). At these bonded interfaces, after multi-fluorescence examination, a rodhamine B-labeled hybrid layer and an adhesive layer completely affected by fluorescein penetration (nanoleakage) through the porous resin-dentin interface, was observed at 24 h evaluation. These samples were labeled using a doubled dye technique, and resulted from combining specific filters after matching the excitation line and the emission band. This technique permits assessing specimens that contain two fluorophores labeling different targets, observing each target separately, or at the same time. The advantage of simultaneous excitation is that the corresponding pixels of the

two images are definitely in register because a single spot of incident light is the source of both of them (Pawley, 2006), allowing the overlapping between both original channels.

When Single Bond (SB) adhesive was applied on PA-etched dentin, the resin was able to diffuse within the porous dentin creating a thick hybrid layer (Figs. 1A, 4A). The dentin interface presented funneled dentinal tubules, more pronounced in sound dentin (Fig. 1A). Funneling is considered an essential sign of degradation of the poorly resin-infiltrated demineralized and peritubular dentin (Profeta et al., 2013). It was pointed out after the evaluation of the fluorophore which labeled the Rhodamine as a separate target, matching the excitation line and the emission band (Pawley, 2006). This advanced degree of degradation may be explicitly attributed to the high hydrophilicity of this interface. The interface may have permitted excessive water adsorption and induced severe resin degradation as well as the extraction of water-soluble unreacted monomers or oligomers from the resin matrix (Tay and Pashley, 2003). Rhodamine B, in the same way, passed along the tubules through the hybrid zone by the interface. Discontinuities in the tubular filling with primer or adhesive were also seen in this single labeled sample. This indicates the intermittent passage of fluorescein from the lateral tubuli toward the main dentinal tubules. Nevertheless, mechanical loading produced a clearly outlined fluorescence due to a consistent Ca-minerals deposited within the bonding interface and inside the dentinal tubules. It was observed earlier after treating with xylenol (Xo-dye) the load cycled sound specimens (Fig. 2D). These findings may be interpreted as dentin remineralization (Toledano et al., 2015a). The Xo dye is commonly employed in bone remineralization studies due to the ability to form complexes with divalent calcium ions (Profeta et al., 2013).

Caries-affected dentin is an active scaffold which facilitates the formation of oriented crystalline hydroxyapatite inside the collagen fibrils (Niu et al., 2014; Nudelman et al., 2010) as crosslinking remained in the caries-affected dentin (Kuboki et al., 1981). Carious dentin specimens treated with PA+SB load cycled put forward severe micropermeability and profuse water sorption at the interface, in spite of the evident reflective signals that represent the presence of mineral components (Fig. 4B). Nevertheless, a relative degree of nanoleakage may correlates with dentin remineralization (Balooch et al., 2008; Hosoya et al., 2010). The zone of demineralization produced by bacterial acids in caries-affected dentin is usually more extensive than the actual zone of bacterial invasion via the dentinal tubules. Thus, dissolution of the peritubular dentin indicates a faster speed of progression of the carious lesion (Chaussain-Miller et al., 2006).

Porosity and nanoleakage diminished after using PA+SB-ZnO without load cycling (Fig. 2A). Both decreased even more after using $ZnCl_2$ (Fig. 2C) or load cycling in the specimens treated with PA+SB-ZnO (Fig. 2B). As a result, evidences of the therapeutic bioactivity of the experimental Zn-bonding agents were attained. Reduced fluorescent-dye uptake (nanoleakage) was observed along the entire resin-dentin interface. These latter observations along with the strong Xo-dye signal from the hybrid layer and the dentinal tubules, clearly indicated the remineralization with biological apatite of those areas which were previously detected as mineral deficient/poor-resin infiltrated zones of the resin-dentin interface. Biological apatite is calcium deficient and contains substantial amounts of carbonate (Fulmer and Brown, 1993). Carbonated apatite is a precursor of HAp. In the presence of zinc an exchange between Zn^{2+} and Ca^{2+} may also occur *in vitro*, forming a substituted apatite compound (Mayer et al., 1994). An isomorphous substitution can be obtained when Ca^{2+} is replaced by Zn^{2+} into

HAp. Scholzite crystals - $CaZn_2(PO_4)_2 \cdot 2H_2O$ - formation in dentin has been previously set out (Osorio et al., 2014a). Mild fluoroscein dye penetration (*i.e.*, micropermeability) and water sorption were pointed out within the resin infiltrated hybrid layer when PA+SB-ZnO without load cycling was used (Fig. 2A). Both figures (2A, 2B) exhibited a discrete spectral overlap (yellow), in the emission of profile of both dyes (red and green), but funneling of the tubular orifices was not evident. The resin-dentin interface was characterized by profuse large-size and funnel-shaped resin tags. Micropermeability was detected several microns away from the adhesive layer (Fig. 2A). On the contrary, a clear micropermeability within the dentinal tubules and at the intertubular dentin was evidenced after using PA+SB-ZnO without load cycling in carious dentin. Nevertheless, any nanoleakage signal from the hybrid layer located underneath the adhesive layer was observable (Fig. 4C). When PA+SB-$ZnCl_2$ (Fig. 2C) was used, fluorescein did not penetrate the entrance of tubules. Furthermore, the thickness of the Rhodamine B-labeled adhesive was not affected by water sorption, but scarce reflective signals from the demineralized dentin layer and inside the dentinal tubules could be observable. Dentinal tubules adopted cylindrical shapes, with a good penetration of the adhesive into the tubules and their lateral branches. This adhesive layer was definitively characterized by the presence of multiple and hermetic resin tags. The diffusion of Rhodamine B along the tubules through the hybrid zone, and along the interface made this adhesive to exhibit the greatest sealing capability. It may be speculated that the highest sealing ability developed by SB-$ZnCl_2$ may be consistent with a slower Zn^{++} liberation rate from ZnO-resin doped. Thus, Ca and P deposits for delayed remineralization will be created, in contrast with $ZnCl_2$-resin doped (Osorio et al., 2014a). In $ZnCl_2$-resin doped specimens, $ZnCl_2$ is not completely mixed within the resin. As a result, clustered nodules of $ZnCl_2$ have seen set out on resin surfaces

(Osorio et al., 2014b) and observed earlier in the present research (Fig. 2C). Salts are strong electrolytes when these ions are dissolve in water. They do so with complete dissociation, determining in this case high and rapid Zn^{2+} dissolution and liberation. Zn^{2+} will bind with free phosphate and precipitate as zinc phosphate crystals. Dissolution rate of $ZnCl_2$ is very fast in comparison with that of ZnO, resulting in higher supersaturation for zinc phosphate (Osorio et al., 2014b). Additionally, in previous publications of Raman analysis, the nature of collagen denoted a rise in crosslinking of collagen that usually results after mineral nucleation (Toledano et al., 2015b) when PA+SB-$ZnCl_2$ was used. This procedure gave rise to the frequently referred improvement of the sealing ability. Opposite outcomes were obtained at the caries-affected dentin substrata treated with PA+SB-$ZnCl_2$ without load cycling (Fig. 4E). In this group, a strong pattern of micropermeability within the dentinal tubules and the adhesive layer, and between the adhesive layer and the resin composite was pointed out. Nevertheless, a limited porosity and brief nanoleakage signal from the hybrid layer located within the labeled adhesive layer infiltrated throughout the intertubular dentin. The lack of sealing ability was appreciated in caries-affected dentin substrata treated with both PA+SB-ZnO and PA+SB-$ZnCl_2$ without the challenge of load cycling. This *in vitro* oral function was, thereby, undertaken to obtain interfaces showing consistent xylenol-stained Ca-deposits within the hybrid layer, walls of dentinal tubules and resin tags when ZnO was used (Fig. 4D). A discrete dye sorption throughout the thickness of the resin adhesive and moderate reflective signal inside the dentinal tubules was unveiled, indicating the presence of some mineral components, when $ZnCl_2$ was employed (Fig. 4F). This means that the sealing capability was not totally achieved by doping with $ZnCl_2$. $ZnCl_2$ is highly acidic (Brown, 2006) soluble and hydrophilic, and added to the adhesive blend, produces and over-etching effect within the infiltrated

dentin, demineralizing even more the underlying carious dentin, just previously and pathologically demineralized (Osorio et al., 2011). Apart from that, it has been clearly demonstrated that intermittent compressive load stimulates the alkaline phosphatase activity. Alkaline phosphatase, present at all mineralization sites, hydrolyzes phosphate esters producing free phosphate, and thus apatite supersaturation (Posner et al., 1986).

3.2. Zn-doped etch-and rinse adhesives, in EDTA treated dentin

Severe fluoroscein dye penetration (*i.e.* micropermeability) and water sorption was observed in specimens of sound dentin treated with EDTA+SB. Minimal nanoleakage was accounted within the resin-infiltrated hybrid layer, after 24 h. This adhesive layer was characterized by the presence of irregular dye accumulation at the resin-dentin interface, no water sorption through the thickness of the adhesive layer, and multiple and short resin tags (Fig. 1B). When this group was submitted to load cycling, CLSM single-projection image disclosing the fluorescent calcium-chelators dye xylenol orange of the resin/sound dentin-interface, revealed strong signals of xylenol orange stain at the top of resin-dentin interface, and within the dentinal tubules. These findings confirmed new mineral precipitation (Profeta et al., 2013) at the hybrid layer and at the first 5-10 μm of the tubule lengths (Fig. 3B). Similarly, when EDTA+SB was used to treat carious dentin, a light pattern of micropermeability within the dentinal tubules and at the hybrid layer, was noticed (Fig. 5A). A generalized porosity and diffuse nanoleakage signal from the hybrid layer (asterisks), located below the B-labeled adhesive layer, infiltrated throughout the intertubular carious dentin. Signals of xylenol orange stain were pointed out at the resin/caries-affected dentin interface, involving multiple dentinal tubules, after load cycling application, as proof of recent mineral formation (Fig. 5B).

Nevertheless, when sound dentin was treated with EDTA+SB-ZnO strong micropermeability between the Rhodamine B-labeled adhesive layer and dentin, localized at the bottom of the hybrid layer, was discovered (Fig. 3A). Severe dye sorption throughout its thickness also appeared at the interface. Fluoroscein dye was accumulated at the entrance of some non-sealed tubules, though some others tubules were resin-filled, and medium-size resin tags were observed. This description was supported by the poor reflective signal, *i.e*, scarce remineralization, detected from the demineralized dentin layer and inside the dentinal tubules (Fig. 3A).

In contrast, when sound (Fig. 3C) or carious (Fig. 5C) specimens were treated with EDTA+SB-$ZnCl_2$ and were not loaded, less micropermeability between the dentin and the adhesive layer was produced, appearing as points of overlapped light spectral (yellow) (Fig. 3C) in the emission profile of red and green dyes. It complies with reduced signs of nanoleakage. On the contrary, profuse water sorption occurred into the labeled adhesive when caries-affected dentin was treated (Fig. 5C). This can lead to dilution of the monomers to the extent that polymerization is inhibited (Jacobsen and Söderholm, 1995), resulting in material swelling (Profeta et al., 2013). Remarked mineral components characterized this interface in sound dentin, as strong reflective signal from the inside of the dentinal tubules were observed earlier (Fig. 3C). In the same way, orange hybrid layer and tubular content denoted new mineral precipitation as result of $ZnCl_2$-doped adhesive at the interface (Fig. 3D). Load cycling applied on specimens treated with EDTA+SB-$ZnCl_2$ did not produce any signs of nanoleakage nor water sorption. A moderate reflective signal from the demineralized dentin layer and inside the dentinal tubules were observed. It indicates the presence of mineral components. In general, no further dye diffused into the adhesive layer (Fig. 5D).

3.3. Zn-doped self-etching adhesives

Considering the self-etching adhesives, SEB applied on smear layer-covered sound dentin created a bonded-dentin interface characterized by limited micropermeability. Hence, scarce both porosities and nanoleakage were observed. The adhesive layer was affected by reduced water sorption and put forward evident resin tags (Fig. 1C). When the interfacial characterization and micropermeability of the resin/sound dentin-interface of SEB·P-$ZnCl_2$ unloaded was analyzed, stronger micropermeability between dentin and the adhesive layer, and within the dentinal tubules, were pointed out (Fig. 6A). A complete nanoleakage signal from the hybrid complex located underneath the adhesive layer. The whole interface and some resin tags exhibited an intense spectral overlap (yellow), in the emission of profile of both dyes (red and green), probably linked to the existence of a partially demineralized layer at the bottom of the hybrid layer. Clearfil SE Bond adhesive system involves a two-step application procedure. SEB·P represents the more fluid and thus probably more chemically active component of SEB system, which is applied first. Most likely, the primer itself may have produced self-assembled nano-layering (Yoshida et al., 2012). This structure is made up of two MDP molecules with their methacrylate groups directed towards each other and their functional hydrogen phosphate groups directed away from each other. In between, the layers calcium salts are deposited and basically hold the layers together. Zn^{++} may causes interaction with MDP forming Zn-MDP complexes when it is combined with the primer (SEB·P-Zn doped) and applied on dentin previous to the adhesive bonding placement (SEB·Bd). This reduced the Ca-MDP salts formation (Osorio et al., 2011). As a consequence, the penetration of free MDP into the partially demineralized dentin is compromised, due to simultaneous formation of MDP-Zn and Ca-MDP-Zn salts rather than MDP-Ca (Feitosa et al., 2014).

On the contrary, load cycling (Fig. 6B) showed a definitive lack of signs of nanoleakage (pointer). In addition, no further dye diffused into the adhesive layer and a strong reflective signal from the bottom of the hybrid complex and inside the dentinal tubules. It indicates the presence of a solid and obliterating mineral segment. These reflective signals correspond with the strong signals of Xo-dye within the hybrid complex and dentinal tubules, even at carious dentin treated with the same adhesive (SEB·P-$ZnCl_2$) load cycled (Fig. 7E). This revealed the presence of calcium complexes within the adhesive structures at both sound and carious substrates (Figs. 6B, 6G, 7E). Their nature probably is phosphate complexes, due to the reaction of MPD, Zn^{++} and Ca^{++} during the application of Zn-doped MPD solution on a calcium-rich dentin surface (Feitosa et al., 2014). Those phosphate complexes probably also became associated with the signals of Xo-dye within the hybrid complex and dentinal tubules that appeared after using ZnO in the primer (SEB·P-ZnO·Xo) (Fig. 6E), or into the bonding (SEB·Bd-ZnO·Xo) (Fig. 6F). When both primer and bonding were ZnO-doped and applied in carious dentin, signals of xylenol orange stain were, similarly, pointed out at the resin-dentin interface, affecting both the hybrid complex (Figs. 7C, 7D) and the entrance of some dentinal tubules (Fig. 7D). ZnO is an amphoteric oxide, although normally shows basic properties (Spero et al., 2000).

Consistent mineral segments within and around the dentinal tubules appeared at the interface, as denoted the strong reflective signals when SEB·Bd-$ZnCl_2$ was applied in sound dentin, and the resin-dentin interface appeared completely sealed without any sight of nanoleakage (Figs. 6C, 6D). As a result, intertubular and peritubular dentin showed a more advanced mineral nucleation, turning up strongly mineralized. When this adhesive was applied on carious dentin, the fluorescence signal from the calcium-chelators dye xylenol orange was localized solely within the dentinal tubules (Fig. 7F).

As a consequence, new mineral segments did not precipitated at the hybrid complex. Micropermeability and nanoleakage were also absent when ZnO was used for doping the primer (Fig. 7A) and the bonding (Fig. 7B) of SEB applied in carious dentin. No further dye diffuses into both adhesive layers. Nevertheless, obliterating mineral segment were more abundant when Zn was included into the bonding, and the sample was load cycled, as fluorescein penetrated less (Fig. 7B). In dentin treated with any zinc-doped mixture of SEB bonding system (SEB·Bd), the remineralization of the bonding interface below the resin-primed demineralized collagen was not affected by the presence of a previous adhesive layer (SEB·P). These Ca-MDP complexes, organized in nano-layering (Yoshida et al., 2012) did not hamper the inward diffusion of ions. These nano-layers helped for further interactions between the remaining Ca^{++} and Zn^{++} ions, the curable resin matrix containing acidic functional, Zn-MDP and Ca-MDP-Zn complexes, and the partially demineralized collagen (Osorio et al., 2011). This lower salt formation, plus the alkalinity promoted after mechanical loading (McAllister and Frangos, 1999) could also account for the less effective liberation of zinc ions at the resin-dentin interface.

The association among the *in situ* liberation of Zn^{++}, mineral precipitation and *in vitro* load cycling on partially demineralized and infiltrated dentin is supported by the effect of compressive loads on the stimulation of the tissue alkaline phosphatase (McAllister and Frangos, 1999). This is a zinc-metalloenzyme that hydrolyzes a broad range of phosphate monoesters (Posner et al., 1986; Price et al., 2009). At high phosphate concentration, calcium pyrophosphate, calcium phosphate and unstable and non-crystalline amorphous complexes are formed (Cheng and Pritzker, 1983) around the collagen fibrils. Dentin keeps the alkaline phosphatase and other enzymes "fossilized" (Van Meerbeek et al., 2001), thus hindering the complete remineralization.

The slower Zn^{2+} liberation rate, from ZnO-doped adhesives, will facilitate the formation of a ZnO rich layer that will permit Ca and P deposits and further remineralization. Higher solubility of ZnO when combined with acids may permit the slow and effective release of zinc ions at the resin-dentin interface when pH is lowered, as it occurs in carious dentin. Zinc might enable to get the balance between dentin demineralization and remineralization processes, from the classic cariostatic effects of fluoride to new-generation of caries-preventive agents (Nyvad et al., 2013).

Though this study represents, to the best of our knowledge, the first to characterize degradation of the Zn-doped resin-dentin interface and morphological structure of sound and carious substrata infiltrated with these resins and submitted to load cycling. New steps for quantifying with numerical data on the ongoing of this research are required. To determine the influence of temperature, to incorporate new techniques as transversal microradiography (TMR) or micro-X-ray diffractometry (μXRD^2) and Transmission Electron Microscopy/selected area diffraction (TEM/SAED deserve future studies in the field of caries-affected dentin therapy.

4. Conclusions

Porosity and nanoleakage did not exist when applying the etch-and-rinse adhesive Single-Bond doped with $ZnCl_2$ in phosphoric acid-treated (PA+SB- $ZnCl_2$) sound dentin. At carious dentin the most hermetic adhesive layer and resin tags resulted after using PA+SB-$ZnCl_2$ and additional load cycling. Nanoleakage and water sorption were not encountered at the SB-$ZnCl_2$-sound dentin interface if previously treated with EDTA.

Load cycling promoted an advanced therapeutic activity in caries-affected dentin treated with EDTA+SB-$ZnCl_2$. When sound dentin surfaces were treated with $ZnCl_2$,

doping the primer or the bonding system of the self-etching system SEB, any porosity nor nanoleakage affected the resin-dentin interface.

Mechanical loading applied on SEB primer doped with ZnO (SEB·P-ZnO) created a solid and extensive platform of new mineral at the resin-dentin interface. Caries-affected dentin treated with ZnO-doped SEB, attained the best sealing, commonly associated to consistent mineral segments at the resin-dentin interface and a generalized intratubular mineralization.

Acknowledgments

This work was supported by the Ministry of Economy and Competitiveness (MINECO) [Project MAT2014-52036-P]. The authors affirm that no actual or potential conflict of interest including any financial, personal or other relationships with other people or organizations within three years of beginning the submitted work that could inappropriately influence, or be perceived to influence, their work. Any other potential conflict of interest is disclosed.

References

Balooch, M., Habelitz, S., Kinney, J.H., Marshall, S.J., Marshall, G.W., 2008. Mechanical properties of mineralized collagen fibrils as influenced by demineralization. J. Struct. Biol. 162, 404–410. DOI:10.1016/j.jsb.2008.02.010

Bertassoni, L.E., Habelitz, S., Kinney, J.H., Marshall, S.J., Marshall, G.W., 2009. Biomechanical perspective on the remineralization of dentin. Caries Res. 43, 70–77. DOI: 10.1159/000201593

Breschi, L., Mazzoni, A., Nato, F., Carrilho, M., Visintini, E., Tjäderhane, L., Ruggeri, A., Tay, F.R., Dorigo, E.D.S., Pashley, D.H., 2010. Chlorhexidine stabilizes the adhesive interface: a 2-year in vitro study. Dent. Mater. 26, 320–325. DOI: 10.1016/j.dental.2009.11.153

Brown, I.D., 2006. The chemical bond in inorganic chemistry; the bond valence model, Oxford University Press, Oxford.

Burwell, A.K., Thula-Mata, T., Gower, L.B., Habelitz, S., Habeliz, S., Kurylo, M., Ho, S.P., Chien, Y.-C., Cheng, J., Cheng, N.F., Gansky, S.A., Marshall, S.J., Marshall, G.W., 2012. Functional remineralization of dentin lesions using polymer-induced liquid-precursor process. PloS One 7, e38852. DOI: 10.1371/journal.pone.0038852

Chaussain-Miller, C., Fioretti, F., Goldberg, M., Menashi, S., 2006. The role of matrix metalloproteinases (MMPs) in human caries. J. Dent. Res. 85, 22–32.

Cheng, P.T., Pritzker, K.P., 1983. Pyrophosphate, phosphate ion interaction: effects on calcium pyrophosphate and calcium hydroxyapatite crystal formation in aqueous solutions. J. Rheumatol. 10, 769–777.

D'Alpino, P.H.P., Pereira, J.C., Svizero, N.R., Rueggeberg, F.A., Pashley, D.H., 2006. Factors affecting use of fluorescent agents in identification of resin-based polymers. J. Adhes. Dent. 8, 285–292.

De Munck, J., Van Landuyt, K., Peumans, M., Poitevin, A., Lambrechts, P., Braem, M., Van Meerbeek, B., 2005. A critical review of the durability of adhesion to tooth tissue: methods and results. J. Dent. Res. 84, 118–132. DOI: 10.1177/154405910508400204

De Oliveira, M.T., Arrais, C.A.G., Aranha, A.C., de Paula Eduardo, C., Miyake, K., Rueggeberg, F.A., Giannini, M., 2010. Micromorphology of resin-dentin interfaces using one-bottle etch&rinse and self-etching adhesive systems on laser-treated dentin surfaces: a confocal laser scanning microscope analysis. Lasers Surg. Med. 42, 662–670. DOI: 10.1002/lsm.20945

Erhardt, M.C.G., Toledano, M., Osorio, R., Pimenta, L.A., 2008. Histomorphologic characterization and bond strength evaluation of caries-affected dentin/resin interfaces: effects of long-term water exposure. Dent. Mater. 24, 786–798. DOI: 10.1016/j.dental.2007.09.007

Feitosa, V.P., Pomacóndor-Hernández, C., Ogliari, F.A., Leal, F., Correr, A.B., Sauro, S., 2014. Chemical interaction of 10-MDP (methacryloyloxi-decyl-dihydrogen-phosphate) in zinc-doped self-etch adhesives. J. Dent. 42, 359–365. DOI: 10.1016/j.jdent.2014.01.003

Fulmer, M.T., Brown, P.W., 1993. Effects of Na2HPO4 and NaH2PO4 on hydroxyapatite formation. J. Biomed. Mater. Res. 27, 1095–1102. DOI: 10.1002/jbm.820270815

Fusayama, T., 1979. Two layers of carious dentin; diagnosis and treatment. Oper. Dent. 4, 63–70.

Göstemeyer, G., Schwendicke, F., 2016. Inhibition of hybrid layer degradation by cavity pretreatment: Meta- and trial sequential analysis. J. Dent. 49, 14-21. DOI: 10.1016/j.jdent.2016.04.007

Griffiths, B.M., Watson, T.F., Sherriff, M., 1999. The influence of dentine bonding systems and their handling characteristics on the morphology and micropermeability of the dentine adhesive interface. J. Dent. 27, 63–71.

Hosoya, Y., Ando, S., Yamaguchi, K., Oooka, S., Miyazaki, M., Tay, F.R., 2010. Quality of the interface of primary tooth dentin bonded with antibacterial fluoride-releasing adhesive. J. Dent. 38, 423–430. DOI: 10.1016/j.jdent.2010.02.001

Jacobsen, T., Söderholm, K.J., 1995. Some effects of water on dentin bonding. Dent. Mater. 11, 132–136. DOI: 10.1016/0109-5641(95)80048-4

Koibuchi, H., Yasuda, N., Nakabayashi, N., 2001. Bonding to dentin with a self-etching primer: the effect of smear layers. Dent. Mater. 17, 122–126.

Kuboki, Y., Tsuzaki, M., Sasaki, S., Liu, C.F., Mechanic, G.L., 1981. Location of the intermolecular cross-links in bovine dentin collagen, solubilization with trypsin and isolation of cross-link peptides containing dihydroxylysinonorleucine and pyridinoline. Biochem. Biophys. Res. Commun. 102, 119–126.

Mayer, I., Apfelbaum, F., Featherstone, J.D., 1994. Zinc ions in synthetic carbonated hydroxyapatites. Arch. Oral Biol. 39, 87–90.

McAllister, T.N., Frangos, J.A., 1999. Steady and transient fluid shear stress stimulate NO release in osteoblasts through distinct biochemical pathways. J. Bone Miner. Res. 14, 930–936. DOI: 10.1359/jbmr.1999.14.6.930

Nikaido, T., Kunzelmann, K.H., Chen, H., Ogata, M., Harada, N., Yamaguchi, S., Cox, C.F., Hickel, R., Tagami, J., 2002. Evaluation of thermal cycling and mechanical

loading on bond strength of a self-etching primer system to dentin. Dent. Mater. 18, 269–275.

Niu, L.N., Zhang, W., Pashley, D.H., Breschi, L., Mao, J., Chen, J.H., Tay, F.R., 2014. Biomimetic remineralization of dentin. Dent. Mater. 30, 77–96. DOI: 10.1016/j.dental.2013.07.013

Nudelman, F., Pieterse, K., George, A., Bomans, P.H.H., Friedrich, H., Brylka, L.J., Hilbers, P.A.J., de With, G., Sommerdijk, N.A.J.M., 2010. The role of collagen in bone apatite formation in the presence of hydroxyapatite nucleation inhibitors. Nat. Mater. 9, 1004–1009. DOI: 10.1038/nmat2875

Nyvad, B., Crielaard, W., Mira, A., Takahashi, N., Beighton, D., 2013. Dental caries from a molecular microbiological perspective. Caries Res. 47, 89–102. DOI: 10.1159/000345367

Osorio, R., Toledano, M., Osorio, E., Aguilera, F.S., Tay, F.R., 2005. Effect of load cycling and in vitro degradation on resin-dentin bonds using a self-etching primer. J. Biomed. Mater. Res. A 72, 399–408. DOI:10.1002/jbm.a.30274

Osorio, R., Yamauti, M., Osorio, E., Román, J.S., Toledano, M., 2011. Zinc-doped dentin adhesive for collagen protection at the hybrid layer. Eur. J. Oral Sci. 119, 401–410. DOI:10.1111/j.1600-0722.2011.00853.x

Osorio, R., Osorio, E., Cabello, I., Toledano, M., 2014a. Zinc induces apatite and scholzite formation during dentin remineralization. Caries Res. 48, 276–290. DOI: 10.1159/000356873

Osorio, R., Cabello, I., Toledano, M., 2014b. Bioactivity of zinc-doped dental adhesives. J. Dent. 42, 403–412. DOI:10.1016/j.jdent.2013.12.006

Pashley, D.H., Tay, F.R., Breschi, L., Tjäderhane, L., Carvalho, R.M., Carrilho, M., Tezvergil-Mutluay, A., 2011. State of the art etch-and-rinse adhesives. Dent. Mater. 27, 1–16. DOI:10.1016/j.dental.2010.10.016

Pawley, J.B., 2006. Handbook of Biological Confocal Microscopy, third ed. Springer, New York.

Posner, A.S., Blumenthal, N.C., Boskey, A.L., 1986. Model of aluminum-induced osteomalacia: inhibition of apatite formation and growth. Kidney Int. Suppl. 18, S17-19.

Price, P.A., Toroian, D., Chan, W.S., 2009. Tissue-nonspecific alkaline phosphatase is required for the calcification of collagen in serum: a possible mechanism for biomineralization. J. Biol. Chem. 284, 4594–4604. DOI: 10.1074/jbc.M803205200

Profeta, A.C., Mannocci, F., Foxton, R., Watson, T.F., Feitosa, V.P., De Carlo, B., R. Mongiorgi, R., Valdré, G., Sauro, S., 2013. Experimental etch-and-rinse adhesives doped with bioactive calcium silicate-based micro-fillers to generate therapeutic resin-dentin interfaces. Dent. Mater. 29, 729–741. DOI: 10.1016/j.dental.2013.04.001

Sauro, S., Osorio, R., Watson, T.F., Toledano, M., 2012. Therapeutic effects of novel resin bonding systems containing bioactive glasses on mineral-depleted areas within the bonded-dentine interface. J. Mater. Sci. Mater. Med. 23, 1521–1532. DOI: 10.1007/s10856-012-4606-6

Sencer, P., Wang, Y., Walker, M.P., Swafford, J.R., 2001. Molecular structure of acid-etched dentin smear layers--in situ study. J. Dent. Res. 80, 1802–1807. DOI:10.1177/00220345010800090601

Seseogullari-Dirihan, R., Mutluay, M.M., Pashley, D.H., Tezvergil-Mutluay, A., 2016. Is the inactivation of dentin proteases by crosslinkers reversible? Dent. Mater. pii: S0109-5641(16)30484-5. DOI: 10.1016/j.dental.2016.09.036 [Epub ahead of print]

Spencer, P., Ye, Q., Park, J., Topp, E.M., Misra, A., Marangos, O., Wang, Y., Bohaty, B.S., Singh, V., Sene, F., Eslick, J., Camarda, K., Katz, J.L., 2010. Adhesive/dentin interface: the weak link in the composite restoration. Ann. Biomed. Eng. 38, 1989–2003. DOI: 10.1007/s10439-010-9969-6

Spero, J.M., Devito, B., Theodore, L. 2000. Regulatory chemicals handbook, Marcel Dekker Inc, New York.

Tay, F.R., Pashley, D.H., 2003. Have dentin adhesives become too hydrophilic? J. Can. Dent. Assoc. 69, 726–731.

Toledano, M., Aguilera, F.S., Yamauti, M., Ruiz-Requena, M.E., Osorio, R., 2013a. In vitro load-induced dentin collagen-stabilization against MMPs degradation. J. Mech. Behav. Biomed. Mater. 27, 10–18. DOI: 10.1016/j.jmbbm.2013.06.002

Toledano, M., Sauro, S., Cabello, I., Watson, T., Osorio, R., 2013b. A Zn-doped etch-and-rinse adhesive may improve the mechanical properties and the integrity at the bonded-dentin interface. Dent. Mater. 29, e142-152. DOI: 10.1016/j.dental.2013.04.024

Toledano, M., Aguilera, F.S., Cabello, I., Osorio, R., 2014a. Remineralization of mechanical loaded resin-dentin interface: a transitional and synchronized multistep process. Biomech. Model. Mechanobiol. 13, 1289–1302. DOI: 10.1007/s10237-014-0573-9

Toledano, M., Cabello, I., Aguilera, F.S., Osorio, E., Toledano-Osorio, M., Osorio, R., 2015a. Improved sealing and remineralization at the resin-dentin interface after

phosphoric acid etching and load cycling. Microsc. Microanal. 21, 1530–1548. DOI: 10.1017/S1431927615015317

Toledano, M., Aguilera, F.S., Osorio, E., Cabello, I., Toledano-Osorio, M., Osorio, R., 2015b. Bond strength and bioactivity of Zn-doped dental adhesives promoted by load cycling. Microsc. Microanal. 21, 214–230. DOI: 10.1017/S1431927614013658

Van Meerbeek, B., Vargas, S., Inoue, S., Yoshida, Y., Peumans, M., Lambrechts, P., et al., 2001. Adhesives and cements to promote preservation dentistry. Oper. Dent. 26, S119-S144.

Yoshida, Y., Yoshihara, K., Nagaoka, N., Hayakawa, S., Torii, Y., Ogawa, T., Osaka, A., Meerbeek B.V., 2012. Self-assembled nano-layering at the adhesive interface. J. Dent. Res. 91, 376–381. DOI: 10.1177/0022034512437375

Figure 1

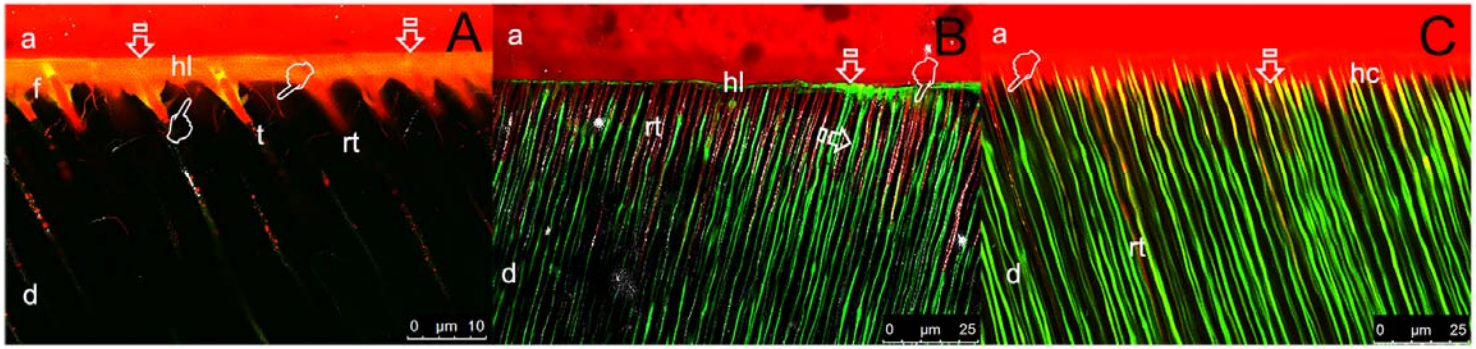

Figure 1. Fig 1A, CLSM image (reflexion/fluorescence) of the resin-sound dentin interface created using PA+SB, after 24 h of storage, showing micropermeability (arrow) between dentin (d) and the adhesive layer (a). An intense nanoleakage signal from the hybrid layer (pointers) (hl) located underneath a thick adhesive layer, may be pointed out. A strong spectral overlap (yellow) in the emission of profile of both dyes (red and green), corresponds with clear signs of nanoleakage. Funnelling (f) of the tubular orifices is observable, with good penetration of the adhesive (a) into the entrance of tubules (t). The adhesive layer is characterized by slight dye sorption throughout its entire thickness and by the presence of long resin tags (rt). (Scale bar: 10 µm). Fig 1B, CLSM image (reflexion/fluorescence) showing the interfacial characterization and

micropermeability, of the resin sound dentin-interface of EDTA+SB, after 24 h of storage. Extensive micropermeability (arrows) between dentin (d) and the adhesive layer (a) is observed. A partial and discrete nanoleakage signal from the hybrid layer (pointer) located underneath a thick adhesive layer is shown. This interface exhibited a light spectral overlap (yellow), in the emission of profile of both dyes (red and green). The adhesive layer is characterized by a null dye sorption throughout its thickness and by the presence of a substantial number of narrow and short resin tags (rt) when imaged in rhodamine excitation/emission mode (Scale bar: 25 μm). Fig 1C, CLSM image (reflexion/fluorescence) showing the interfacial characterization and micropermeability of the resin sound dentin-interfaces of SEB, after 24 h of storage, displaying micropermeability (arrow) between dentin (d) and the adhesive layer (a). A partial nanoleakage signal from the hybrid complex (pointer) (hc) located underneath the adhesive layer may be pointed out. The adhesive layer characterized by a tight dye sorption throughout its thickness and by the presence of thin resin tags (rt) when imaged in rhodamine excitation/emission mode (Scale bar: 25 μm). a, adhesive layer; d, dentin; f, funneling; hc, hybrid complex; hl, hybrid layer; rt, resin tags; t, dentinal tubules.

Figure 2

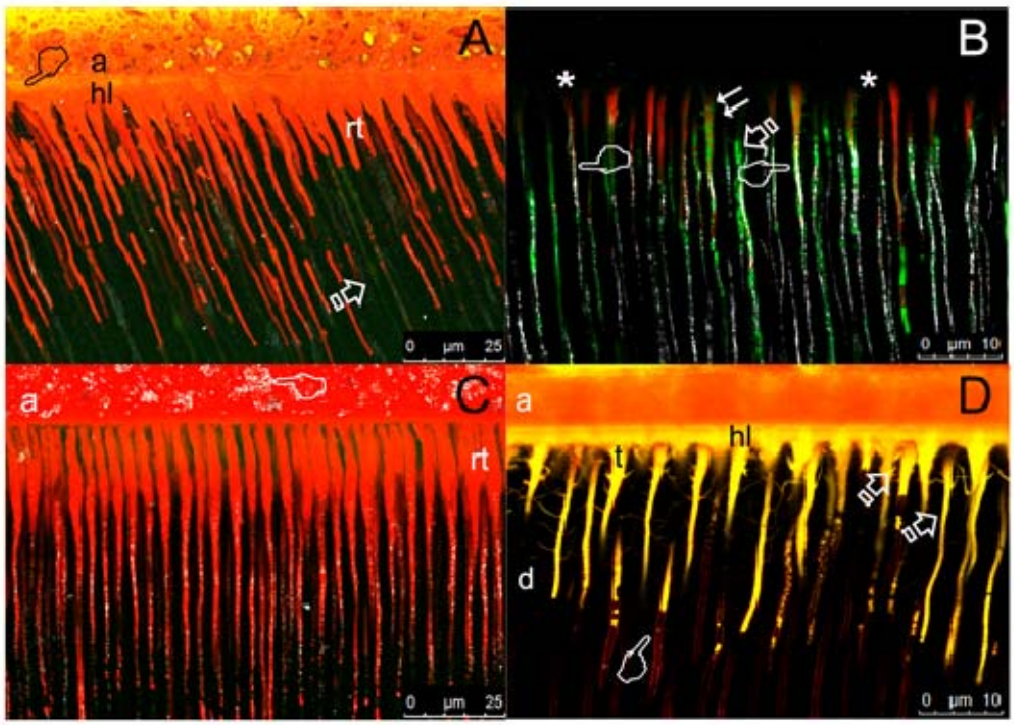

Figure 2. CLSM images (reflexion/fluorescence) showing the interfacial characterization and micropermeability of the resin/sound dentin interface created using phosphoric acid and Single Bond adhesive-ZnO doped (PA+SB-ZnO) without load cycling (A), PA+SB-ZnO load cycled (B), PA+SB-$ZnCl_2$ without load cycling (C), and PA+SB load cycled with dye xylenol orange (PA+SB·Xo) (D). A weak pattern of micropermeability within the dentinal tubules (arrow), and between the Rhodamine B-labeled adhesive layer (a) and the hybrid layer (hl) may be observed at Fig 2A, exhibiting a light spectral overlap (yellow) (pointer) in the emission of profile of both dyes (red and green). Wider funnel-shaped resin tags (rt) underneath the adhesive layer characterize the resin-dentin interface (Scale bar: 25 µm). Fig 2B unveils a complete absence of signs of nanoleakage (asterisks) and a strong reflective signal inside the dentinal tubules, indicating the presence of mineral components (pointers). Continuous

(arrow) or intermittent (double arrows) fluorescein dye permeates. No further dye diffuses into the adhesive layer, and shorter or thinner resin tags are detected (Scale bar: 10 μm). A definitive lack of signs of nanoleakage is characterized at Fig 2C, where both null penetration of fluoroscein throughout the proximal ends of dentinal tubules and water sorption within the thickness of the Rhodamine B-labeled adhesive (a) can be seen. Clustered nodules of $ZnCl_2$ are pointed out at the adhesive layer (pointer). Deep and scarce reflective signals from the demineralized dentin layer and inside the dentinal tubules appeared at the interface, where longer and robust resin tags (rt) may be observed (Scale bar: 25 μm). Figs 2B and 2D exhibits mineral deposition visualized within the hybrid layer (hl) and along the dentinal tubules (arrows) (Fig 2D, scale bar: 10 μm). Note the presence of intact resin tags imaged in Rhodamine excitation/emission mode (pointer). a, adhesive layer; d, dentin; hl, hybrid layer; rt, resin tags.

Figure 3

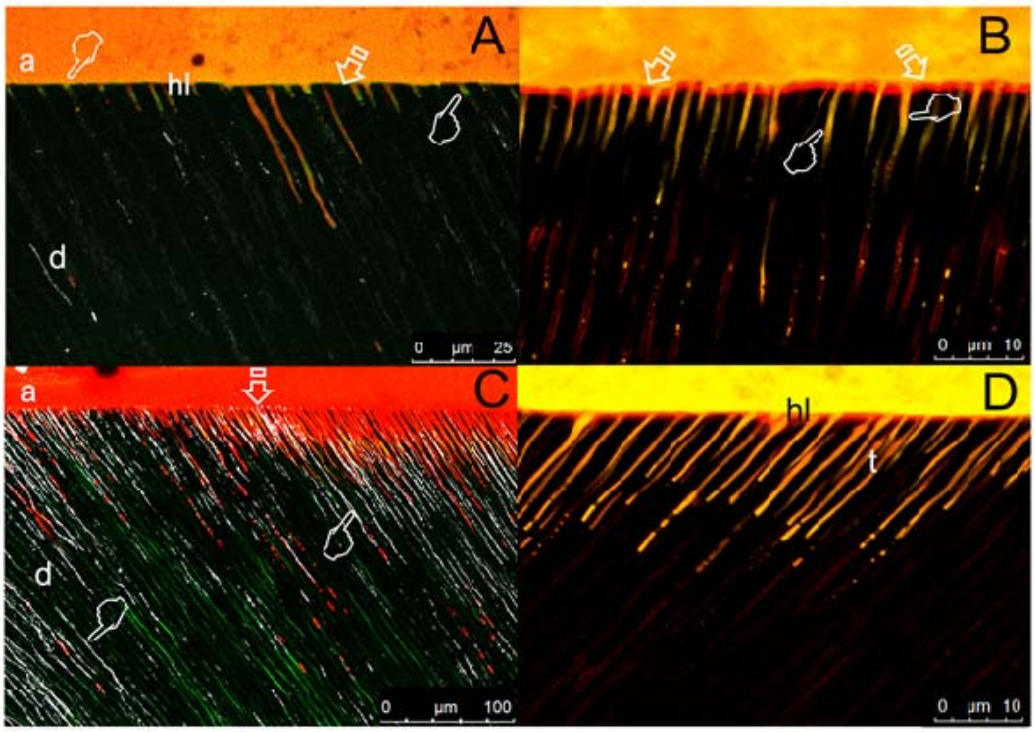

Figure 3. CLSM images (reflexion/fluorescence) showing the interfacial characterization and micropermeability of the resin/sound dentin-interfaces created using EDTA+SB-ZnO unloaded (A), EDTA+SB load cycled with dye xylenol orange (EDTA+SB·Xo) (B), EDTA+SB-$ZnCl_2$ unloaded (C), and EDTA+SB-$ZnCl_2$ unloaded with dye xylenol orange (EDTA+SB-$ZnCl_2$·Xo) (D). Fig 3A is showing strong micropermeability between the Rhodamine B-labeled adhesive layer (a) and dentin (d) (arrow), specially localized at the bottom of the hybrid layer. Severe dye sorption throughout its thickness is discovered. Fluoroscein dye results accumulated at the entrance of tubules (pointers). Some long and a substantial number of short resin tags are pointed out. Poor reflective signal from the demineralized dentin layer and inside the dentinal tubules is detected (Scale bar: 25 µm). Fig 3B is showing a CLSM single-projection image disclosing the fluorescent calcium-chelators dye xylenol orange of the resin/sound dentin-interface created using EDTA+SB-ZnO load cycled. Signals of

xylenol orange stain are observed at the top of resin-dentin interface (arrows), and within the dentinal tubules (pointers) (Scale bar: 10 μm). Fig 3C is showing a CLSM image (reflexion/fluorescence) of the resin-dentin interface created using EDTA+SB-$ZnCl_2$ unloaded, showing minimal micropermeability (arrow) between dentin (d) and the adhesive layer (a). It appears as points of light spectral overlap (yellow) in the emission of profile of both dyes (red and green), and complies with reduced signs of nanoleakage. Strong reflective signal from the inside of the dentinal tubules may be pointed out (pointers), indicating the presence of mineral components (Scale bar: 100 μm). Fig 3D shows a CLSM single-projection image disclosing the fluorescent calcium-chelators dye xylenol orange of the resin/sound dentin-interface created using EDTA+SB-$ZnCl_2$ without load cycling. The interface discloses a clear fluorescence signal within the dentinal tubules (t) and some areas of the hybrid layer (hl) (Scale bar: 10 μm). a, adhesive layer; d, dentin; hl, hybrid layer; t, dentinal tubules.

Figure 4

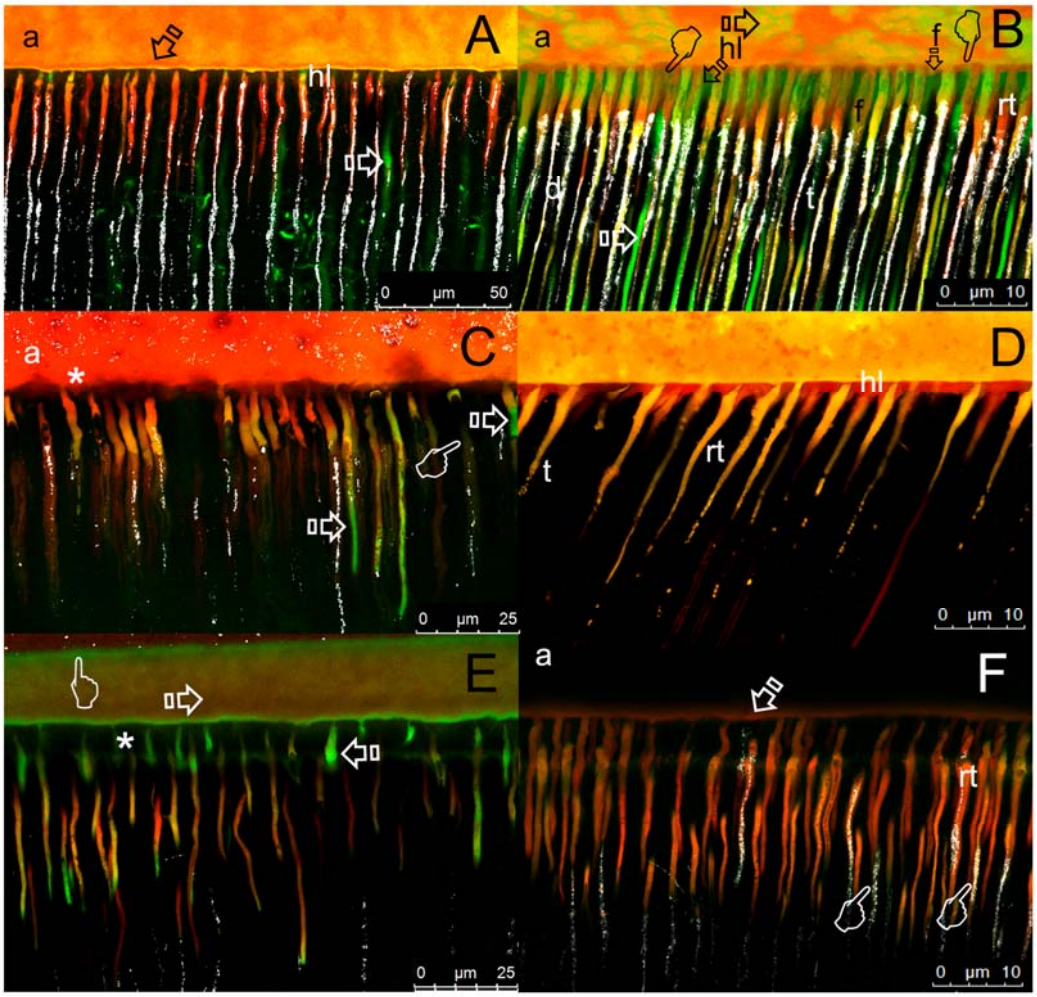

Figure 4. CLSM images (reflexion/fluorescence) showing the interfacial characterization and micropermeability of the resin/caries-affected dentin interface created using phosphoric acid and Single Bond adhesive (PA+SB) unloaded (A), PA+SB load cycled (B), ZnO-doped unloaded (PA+SB-ZnO) (C), ZnO-doped load cycled with dye xylenol orange (PA+SB-ZnO·Xo) (D), $ZnCl_2$-doped unloaded (PA+SB-$ZnCl_2$) (E), and $ZnCl_2$-doped load cycled (PA+SB-$ZnCl_2$) (F). Figs 4A and 4B show a generalized pattern of severe micropermeability and water sorption (arrows), more pronounced in 4B, at both adhesive layer (a) and dentinal tubules (t). A porous hybrid layer and a strong nanoleakage signal from the hybrid layer (pointers) located underneath the Rhodamine B-labeled adhesive layer may be observed (Fig 4B). In the

CLSM image, it is possible to set out an adhesive layer characterized by the presence of a substantial number of wide and long resin tags (rt) underneath the adhesive layer and a profuse dye sorption throughout its thickness. Some resin tags exhibited an intense spectral overlap (yellow), in the emission of profile of both dyes (red and green). Funnelling (f) of the tubular orifices is observable, with good penetration of the adhesive (a) into the entrance of tubules (t), and a moderate reflective signal from the demineralized dentin layer and inside the dentinal tubules indicates the presence of mineral components (Fig 4A, scale bar: 50 μm; Fig 4B, scale bar: 10 μm). A limited and diffuse micropermeability within the dentinal tubules (arrows) or at the intertubular dentin (pointer) is observable, but any nanoleakage signal from the hybrid layer located underneath the adhesive layer (asterisk) could be detected at Fig 4C (Scale bar: 25 μm). Fig 4D shows a CLSM single-projection image disclosing the fluorescent calcium-chelators dye xylenol orange of the resin-dentin interface created with PA+SB-ZnO and load cycled. A clear fluorescence signal due to consistent presence of xylenol-stained Ca-deposits within the hybrid layer (hl), walls of dentinal tubules (t) and resin tags (rt) is unveiled (Scale bar: 10 μm). The interfacial characterization and micropermeability of the resin-dentin interface created using PA+SB-$ZnCl_2$ unloaded is shown at CLSM images (reflexion/fluorescence), and included in Fig 4E. A clear pattern of micropermeability within the dentinal tubules and the adhesive layer (arrows), and between the adhesive layer and the resin composite (pointer) may be pointed out. A limited porosity and brief nanoleakage signal from the hybrid layer (asterisk) located within the labeled adhesive layer infiltrated throughout the intertubular dentin is shown (Scale bar: 25 μm). At the CLSM image of Fig 4F, it is possible to observe a resin-dentin interface characterized by the presence of long-sized funnel-shaped resin tags (rt) underneath the adhesive layer (a) and a discrete dye sorption throughout its thickness

(arrow). A moderate reflective signal inside the dentinal tubules (pointers) indicates the presence of some mineral components (Scale bar: 10 μm). a, adhesive layer; d, dentin; f, funneling; hl, hybrid layer; rt, resin tags; t, dentinal tubules.

Figure 5

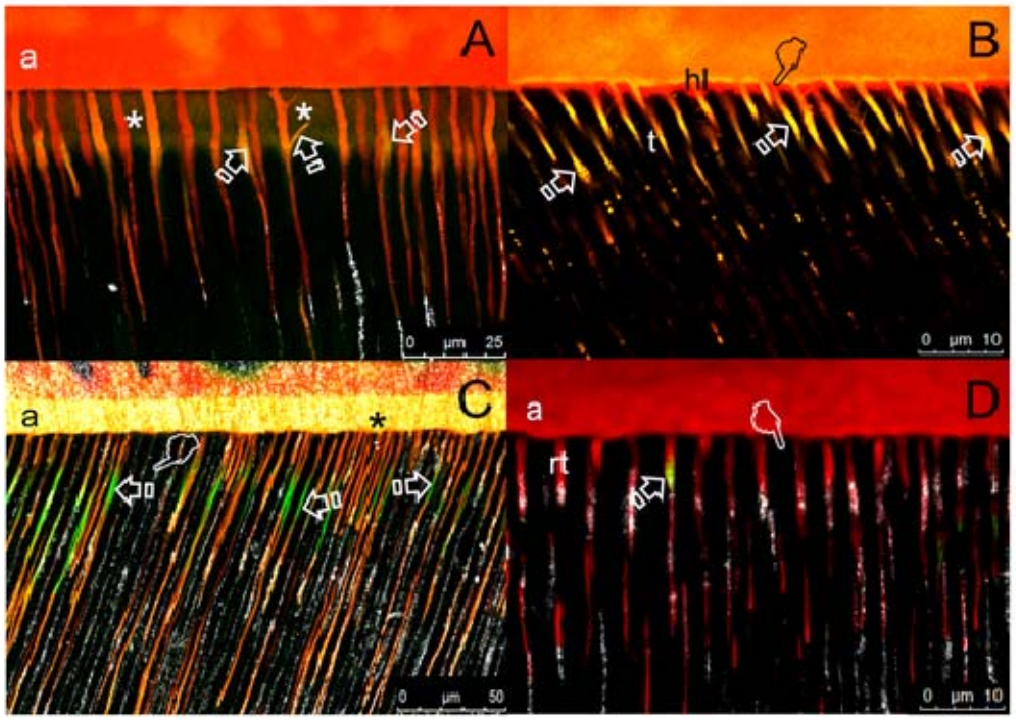

Figure 5. The interfacial characterization and micropermeability of the resin/caries-affected dentin interface created using EDTA and Single Bond adhesive, unloaded, is shown at CLSM images (reflexion/fluorescence), at Fig 5A, where a light pattern of micropermeability within the dentinal tubules (arrows) and at the hybrid layer, may be noticed. A limited porosity and diffuse nanoleakage signal from the hybrid layer (asterisks), locates below the B-labeled adhesive layer, infiltrating throughout the intertubular carious dentin (Scale bar: 25 μm). Fig 5B, obtained at 63x-2 optical zoom with 10 μm of scale bars, shows a CLSM single-projection image disclosing the

fluorescent calcium-chelators dye xylenol orange of the resin-dentin interface created with EDTA+SB load cycled. Signals of xylenol orange stain are pointed out at the resin/caries-affected dentin interface, involving multiple dentinal tubules (t) (arrows). The hybrid layer (hl) appears totally infiltrated with the B-labeled adhesive resin (pointer). Long resin tags are discernible underneath the adhesive layer and hybrid layer (Scale bar: 10 μm). Interfacial characterization and micropermeability of the resin-dentin interface created using EDTA+SB-$ZnCl_2$ without load cycling may be shown at the CLSM images (reflexion/fluorescence) in Fig 5C. A generalized pattern of severe micropermeability between different segments of some resin tags are adverted (arrows), caused by permeability from lateral tubules or from unsealing resin tags. Some resin tags exhibit an intense spectral overlap (yellow), in the emission of profile of both dyes (red and green). The presence of a large number of long-size resin tags is also characteristic. A porous hybrid layer and a moderate nanoleakage signal from the hybrid layer located underneath the Rhodamine B-labeled adhesive layer (pointer), with a profuse dye sorption throughout its thickness may be observed (asterisk) (Scale bar: 50 μm). When EDTA+SB-$ZnCl_2$ load cycling is employed (Fig 5D), a resin-dentin interface imaged in reflexion/fluorescence shows some both absence signs of nanoleakage and water sorption (pointer) and a moderate reflective signal from the demineralized dentin layer and inside the dentinal tubules, indicating the presence of mineral components. No further dye diffuses into the adhesive layer (a), but localized tubular micropermeability was detected at some tubular spot (arrow), as scarce penetration of fluoroscein throughout the dentinal tubules is confirmed. Shorter or thinner resin tags are also detected at the interface (Scale bar: 10 μm). a, adhesive; hl, hybrid layer; t, dentinal tubules.

Figure 6

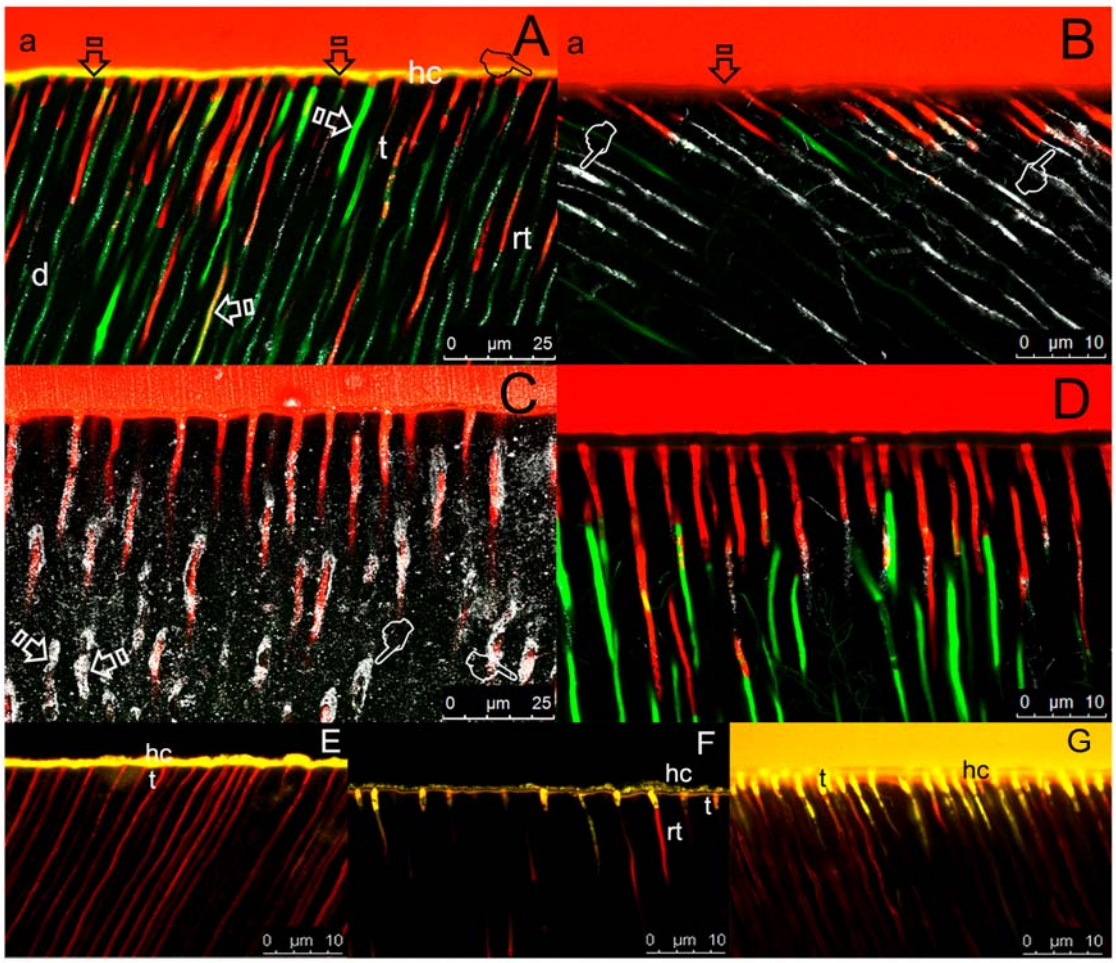

Figure 6. 6A, CLSM image (reflexion/fluorescence) obtained at 63x with 25 µm of scale bar, showing the interfacial characterization and micropermeability, of the resin/sound dentin-interface of SEB·P-$ZnCl_2$, unloaded. Evident micropermeability (arrows) between dentin (d) and the adhesive layer (a), and within the dentinal tubules (t), is shown. A clear nanoleakage signal from the hybrid complex (hc) (pointer), located underneath adhesive layer may be pointed out. The whole interface and some resin tags exhibit an intense spectral overlap (yellow), in the emission of profile of both dyes (red and green). The adhesive layer is characterized by a null dye sorption throughout its thickness. Thin and long resin tags (rt) typify the interface (Scale bar: 25 µm). Fig 6B is showing a resin/sound dentin interface of SEB·P-$ZnCl_2$, load cycled,

imaged in reflexion/fluorescence showing a definitive lack of signs of nanoleakage (arrow). No further dye diffuses into the adhesive layer and a strong reflective signal from the bottom of the hybrid complex and inside the dentinal tubules (pointers) may be observed, indicating the presence of a solid and obliterating mineral segment. Short resin tags are put forward. The fluorescein penetration stops several microns away from the resin-dentin interface (Scale bar: 10 μm). Figs 6C (obtained at 63x with 25 μm of scale bar) and 6D show images (reflexion/fluorescence) of the interfacial characterization and micropermeability, of the resin/sound dentin-interface of SEB·Bd-$ZnCl_2$, unloaded (C) and load cycled (D). Multiple and consistent mineral segments within the dentinal tubules (arrows), or surrounding the lumen of tubules (pointers) appear at the interface, as denoted the strong reflective signals. The fluoroscein penetration does not reach the resin-dentin interface that appeared completely sealed without any sight of nanoleakage. Some resin tags, thin and short, exhibit a clear spectral overlap (yellow) in the emission of profile of both dyes, red and green (Fig 6C, scale bar: 25 μm; Fig 6D, scale bar: 10 μm). Figs 6E, 6F, 6G refer CLSM single-projection images disclosing the fluorescent calcium-chelators dye xylenol orange, showing the interfacial characterization of the resin/sound dentin interface created using SEB·P-ZnO (SEB·P-ZnO·Xo) (E), SEB·Bd-ZnO (SEB·Bd-ZnO·Xo) (F), and SEB·Bd-$ZnCl_2$ (SEB·Bd-$ZnCl_2$·Xo) (G) on smear layer-covered dentin and then load cycled. The adhesive layer is characterized by the presence of thin (E), scarce (F) or multiple and continuous (G) resin tags, when imaged in Rhodamine excitation/emission mode. Intense (E), or moderate (F, G) fluorescence signal of Xo-dye within the hybrid complex (hc), but weak (E, F) or strong (G) signal of Xo-dye within the dentinal tubules (t), reveal the presence of calcium complexes within both adhesive structures (Fig 6E,

scale bar: 10 µm; Fig 6F, scale bar: 10 µm; Fig 6G, scale bar: 10 µm). a, adhesive layer; d, dentin; hc, hybrid complex; rt, resin tags; t, dentinal tubules.

Figure 7

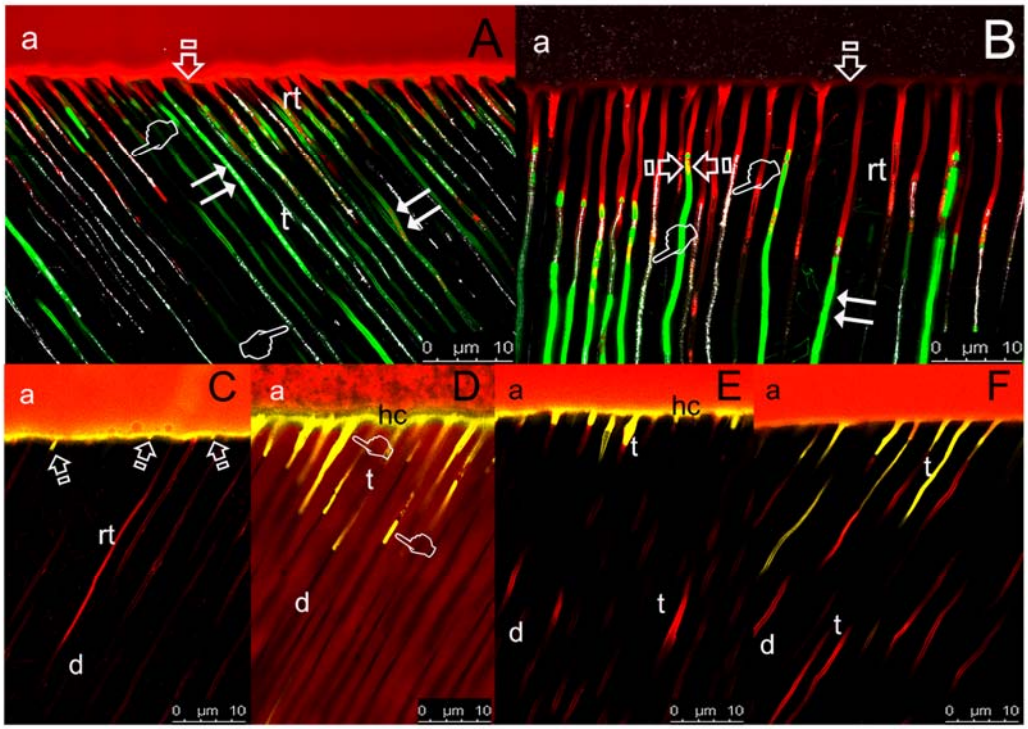

Figure 7. Figs 7A and 7B are showing a CLSM image (reflexion/fluorescence) of the interfacial characterization and micropermeability of the resin/carious-affected dentin-interface of SEB·P-ZnO unloaded (A) and SEB·Bd-ZnO load cycled (B), respectively. Any micropermeability and nanoleakage (arrow) between dentin (d) and the adhesive layer (a), but within the dentinal tubules (t) (double arrows), is shown. No further dye diffuses into the adhesive layer and a strong reflective signal inside the dentinal tubules (pointers), indicating the presence of obliterating mineral segment, are adverted. Some resin tags exhibit an intense spectral overlap (yellow), in the emission of profile of both dyes (red and green) (faced arrows). Thin and short resin tags (rt) are also pointed out (Fig 7A, scale bar: 10 µm; Fig 7B, scale bar: 10 µm). Figs 7C and 7D show a CLSM

single-projection image disclosing the fluorescent calcium-chelators dye xylenol orange. It is shown the interfacial characterization of the resin/caries-affected dentin interface created using SEB·P-ZnO (C) or SEB·Bd-ZnO (D) adhesive applied on smear layer-covered dentin, and then load cycled, imaged in Rhodamine excitation/emission and calcium-chelators dye xylenol orange modes (SEB·P-ZnO·Xo, SEB·Bd-ZnO·Xo). Signals of xylenol orange stain are observed at the resin-dentin interface, affecting both the hybrid complex (hc) and the entrance of some dentinal tubules (arrows) (C), or longer trajectory (D) within the tubules (t) (pointers). Images in Rhodamine excitation/emission mode, permit to point out some long resin tags underneath the adhesive layer and hybrid complex (Fig 7C, scale bar: 10 μm; Fig 7D, scale bar: 10 μm). Figs 7E and 7F are showing CLSM single-projection images disclosing the fluorescent calcium-chelators dye xylenol orange. The interfacial characterization of the resin/caries-affected dentin interface created using SEB·P-$ZnCl_2$ (E) and SEB·Bd-$ZnCl_2$ (F) adhesives applied on smear layer-covered dentin, and then load cycled, imaged in Rhodamine excitation/emission and calcium-chelators dye xylenol orange modes (SEB·P-$ZnCl_2$·Xo, SEB·Bd-$ZnCl_2$·Xo). The interfaces disclose a clear fluorescence signal within the hybrid complex (hc) and dentinal tubules (t). Xo-dye penetrates, in general, the first 5 μm of resin tags when the primer was Zn-doped (E), and longer extent when the bonding was Zn-doped (F) (Fig 7E, scale bar: 10 μm; Fig 7F, scale bar: 10 μm). The rest of resin tags-length appeared with the characteristic Rhodhamine B-labeled colorant. All figures were obtained at 63x-2 with optical zoom at 10μm of scale bar. a, adhesive layer; d, dentin; hc: hybrid complex; rt, resin tags; t, dentinal tubules.